Formation and remediation simulation of an in-situ reactive zone with nanoiron for a nitrobenzene-contaminated aquifer

Li Hui and Zhang Xue-qing

ABSTRACT

A two-dimensional simulated sand box was built to investigate the formation and remediation of an in-situ reactive zone (IRZ) of nanoscale zero-valent iron (NZVI) for a nitrobenzene-contaminated aquifer, and the permeability change of the zone was calculated through the loss of waterhead. The experimental results demonstrated that the remediation area in coarse sand was obviously larger than that in fine sand. The nitrobenzene concentration reached a stable level of 87.24 and 170.24 mg/L in coarse and fine sand by 50 d and 40 d, respectively; after 60 d, the concentration of aniline as the reduction end-product of nitrobenzene was 97.02 and 49.40 mg/L, corresponding to a mean production rate of 40.1% and 20.8%, respectively. This indicated that a wider zone will be formed in the media with a larger size, which is beneficial for pollution remediation. The water yield of the aquifer declined by 13.8% and 11.9% in coarse and fine sand after 60 d, and the final permeability constant was 22.94 and 1.82 m/d (declining by 60.9% and 70.6%), respectively. The reactive zone remained stable and the injection of NZVI slurry could not cause any dramatic changes in the aquifer permeability.

Key words | in-situ reactive zone, nanoscale zero-valent iron, nitrobenzene, permeability, remediation

Li Hui
Zhang Xue-qing (corresponding author)
The Institute of Hydrogeology and Environmental Geology,
Chinese Academy of Geological Sciences,
Shijiazhuang 050061,
China
and
Key Laboratory of Groundwater Remediation of Hebei Province and China Geological Survey,
Shijiazhuang 050061,
China
E-mail: *490838658@qq.com*

INTRODUCTION

As a type of raw material commonly used in modern agriculture, medicine, and chemistry, nitro-aromatics are accumulating substantially in the environment as industrial development continues (Dubey *et al.* 2014; Yan *et al.* 2017). Due to the existence of nitrofunctional groups, the degradation of nitro-aromatics is quite difficult and so they pose a higher toxicity risk to plants and humans than other monocyclic aromatic compounds (Kulkarni & Chaudhari 2007; Rezaei-Vahidian *et al.* 2017). In recent years, the groundwater pollution resulting from nitro-aromatics has drawn widespread public concern, and so a series of engineering technologies, such as microbial remediation (Kulkarni & Chaudhari 2007; Grube *et al.* 2008), chemical oxidation/reduction (Yuan *et al.* 2012; Guria *et al.* 2016), and permeable reactive barriers (Yuan *et al.* 2013; Yin *et al.* 2015), have been tried with the goal of pollution remediation. These methods, however, often need large construction, high costs, and a long period for construction, all of which greatly limit their application in the field (Liu *et al.* 1981; Higgins & Olson 2009).

The in-situ reactive zone (IRZ) has recently emerged as a new type of in-situ remediation technology. One or more IRZs may be created, in the pollution plume, by injecting chemical reactants or microorganisms underground to intercept, immobilize, or thoroughly degrade the target pollutants (Suthersan 2002). Hence, the key to this technique's success is that a reasonably appropriate reactant is chosen according to the pollutant's characteristics. As a

doi: 10.2166/ws.2018.034

reductive metallic material with a very small particle size, and thus a larger specific surface area, and a higher reactivity and reducibility than iron powder (Elliott & Zhang 2001), nanoscale zero-valent iron (NZVI) can effectively degrade various persistent organic pollutants in the environment, such as chlorinated hydrocarbons (Schlicker *et al.* 2000; Zhou *et al.* 2015), heavy metals (Ponder *et al.* 2000), and pesticides (Han *et al.* 2016), among others.

However, due to their size effect and high surface free energy, the iron nanoparticles tend to aggregate in an aqueous medium (Adeleye *et al.* 2013). Therefore, surface modification by some macromolecular materials to enhance the dispersion of nanoiron before its use is necessary. The excellent performance by rare or modified nanoiron in the degradation of nitro-aromatics has been confirmed in several recent studies. Dong *et al.* (2015) prepared emulsified nanoiron for nitrobenzene (NB) degradation and found that the nanoparticles could provide for significant removal of nitrobenzene through adsorption and reductive reaction, with aniline as the end-product. Similarly, another study used NZVI to remove parachloronitrobenzene, finding that the efficiency could reach 98.8% under the condition of pH 2 in 120 minutes (Dong *et al.* 2010). Lin *et al.* (2013) investigated the decomposition of n-nitrodimethylamine (NDMA) in water by using NZVI in the presence of aluminum and iron salts, which removed up to 87.3% of NDMA. Therefore, these studies confirm NZVI could be used as a high-efficiency reactant in the IRZ to remediate groundwater pollution. Generally, however, current study of NZVI tends to mainly focus on its reaction mechanism at the laboratory batch scale (Li *et al.* 2013), or its transport behavior through columns (Tiraferri & Sethi 2009). Hence, we still lack research on IRZ with NZVI, on the actual removal efficiency of nitro-aromatics in the aquifer, and on the permeability change of IRZ during the remediation process. These research avenues are perhaps more practical and applicable for site engineering and are worthy of study.

Given this context, a two-dimensional simulation experiment of in-situ remediation for nitrobenzene pollution was carried out in this study, which had three objectives: (1) to confirm the remediation ability of nitrobenzene by IRZ with NZVI in a simulated aquifer; (2) to study the formation and development of IRZ according to the degradation of nitrobenzene; and (3) to investigate whether the blockage of IRZ resulting from the reduction reaction will appear. Fulfilling all of these should provide a sound basis for the application of IRZ with NZVI for in-situ remediation.

MATERIALS AND METHODS

Experimental materials and setup

NZVI particles were prepared by a chemical reduction method in aqueous solution (He & Zhao 2005). To reduce the particle aggregation and improve their dispersibility, sucrose was chosen as the disperser for preparing the modified NZVI (SM-NZVI). In our previous study, transmission electron microscopy (TEM) images showed that the particle size of prepared SM-NZVI was *c.*100–150 nm with a characteristic diffraction peak at 44.7 °C in the X-ray diffraction (XRD) pattern that represents the α–Fe of the body-centered cubic. The prepared NZVI particles were washed by anhydrous ethanol and deionized water to remove surface impurities, then diluted with water to a fixed concentration for use.

The media materials used for the simulated aquifer were collected from a sandpit in Changchun. The sand was dried in the shade and put through a series of graded sieves ranging in grain size from 0.5–1 mm and 0.1–0.25 mm. Nitrobenzene of analytical grade was purchased from Xinlu Chemical Technology Co., Ltd (Tianjin, China). Several key physical and chemical properties of the sand and the prepared NB-contaminated water are listed in Tables 1 and 2, respectively.

The sand box for the two-dimensional simulation was 130 cm in length, 30 cm in width, and 60 cm in height. There were 60 sample connections on the front of the box, which are expressed by circles in Figure 1. Water distribution boards were installed on the inlet side and outlet side to ensure a uniform media saturation by water. Piezometer tubes (PT) were connected through latex tubing to the sample outlets of the second row and fixed vertically onto the box. Five injection wells, each with a 2 cm internal diameter and all-over holes, were installed in the bottom of the box and *c.*2 cm away from the left water distribution board (wells were 5 cm apart).

Table 1 | Physical and chemical properties of the sand used to simulate an aquifer

Media	Grain size (mm)	pH	Moisture content (%)	Fe^{2+} (mg/kg)	Fe^{3+} (mg/kg)	Permeability coefficient (m/d)
Coarse sand	0.5–1	7.11	0.46	48	153	69.98
Fine sand	0.1–0.25	7.08	0.38	59	196	10.29

Table 2 | Parameters of the experimental contaminated water (unit: mg/L)

NB	pH	ORP (mv)	DO	Ca^{2+}	Mg^{2+}	Fe^{3+}	Fe^{2+}	HCO_3	Cl^-	NO_3^-
400	6.59	−11	8.62	32.63	25.11	153	0.05	105.62	102.21	0.58

Experimental method

To serve as the media of different simulated aquifers in two boxes, coarse sand (245 kg) and fine sand (256 kg) were filled into the box and both pressed layer-by-layer to a height of 42 cm, which corresponded to a volume weight of 1.62 and 1.69 g/cm^3, respectively. To reduce the volatilization loss of NB, some clay was placed on the top of the sand to a depth of 2.5 cm to form an unsaturated zone. Afterwards, NB solution of fixed concentration was slowly introduced into the aquifer via peristaltic pumps until the NB concentration of the outflow was consistent with that of the inflow. Tap water replaced the NB solution as groundwater, which flowed at 0.23 m/d and 0.15 m/d in the coarse and fine sand, respectively; their corresponding permeability coefficients, as calculated through the inlet and outlet water level, were 56.1 m/d and 6.1 m/d. During the next 5 days, prepared 5 L SM-NZVI slurry of 10 g/L was injected into the simulated aquifer via injection wells five times at the same volume. Samples of simulated groundwater were taken regularly to determine the concentrations of NB and aniline (AN) as the end-products.

RESULTS AND DISCUSSION

Removal effect of nitrobenzene in sand boxes

The changing NB concentration in coarse sand is shown in Figure 2. It is evident that the NB concentration significantly declined at the bottom of the injection wells once all the slurry had been injected, and the result indicates that a portion of NB was effectively degraded by SM-NZVI. The flowing groundwater has a limited attenuation effect on

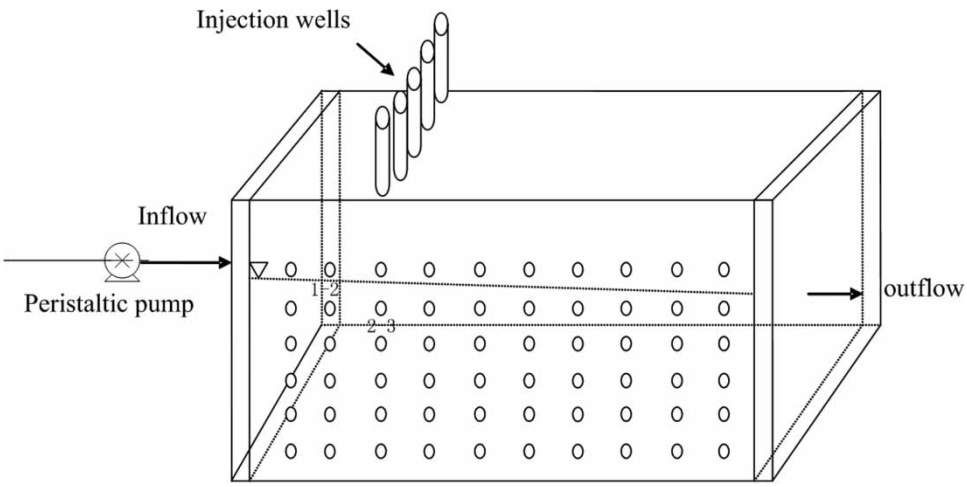

Figure1 | Schematic diagram of the experimental setup (the circles represent sample outlets and the figures such as 1–2 are the row and column numbers of the outlet's position).

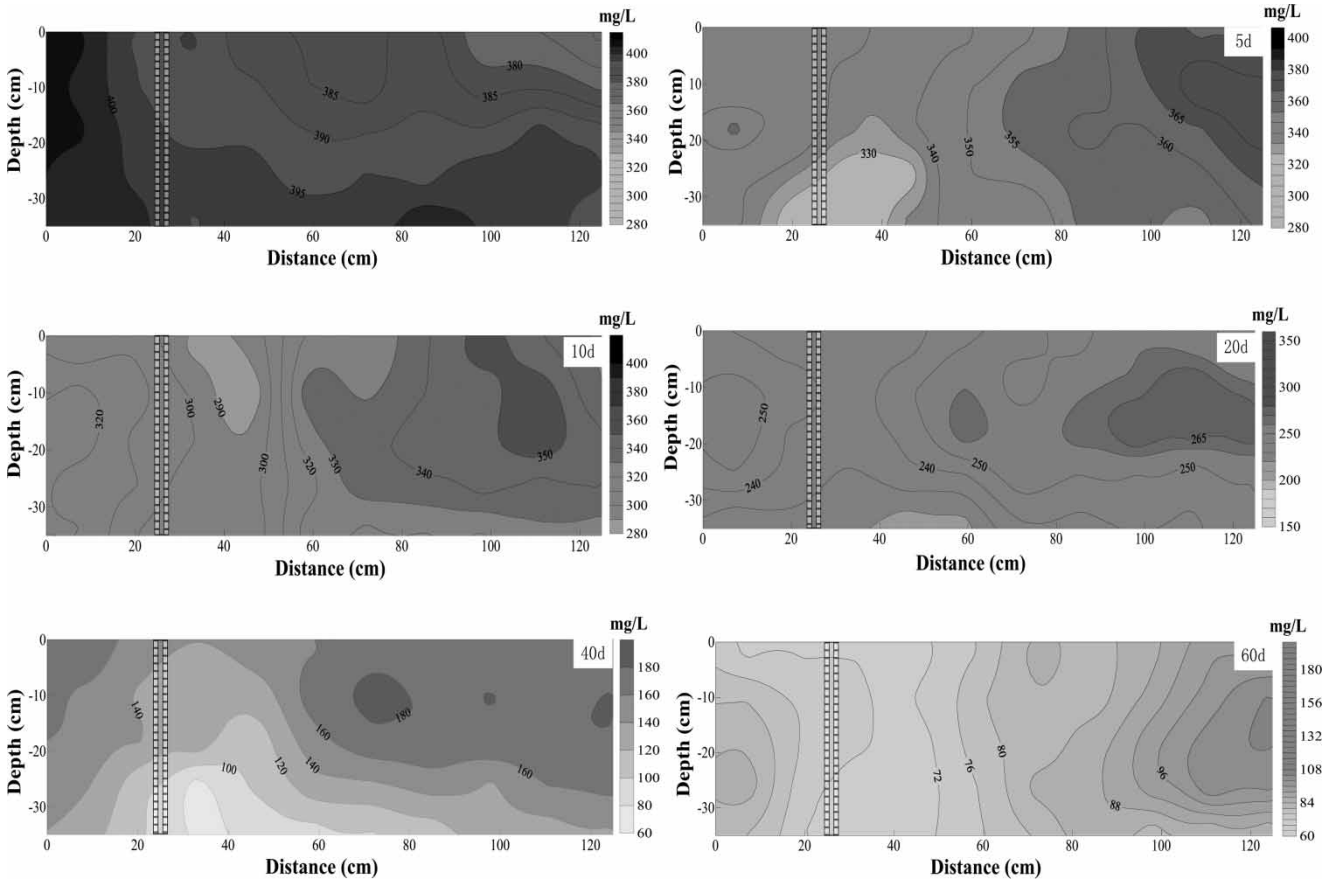

Figure 2 | Concentration change of nitrobenzene in coarse sand.

NB, which is likely negligible when considering NB hydrophobicity and the lower flow velocity of groundwater. In subsequent days, the NB concentration decreased rapidly in the area surrounding the injection wells that could be regarded as the IRZ of SM-NZVI. As shown in Figure 2, the reactive zone occurred in the 15–55 cm portion of the box on the 5th day, and it extended in the direction of the flow, thus bringing about an extensive reactive range of 20–100 cm by the 60th day. Furthermore, due to the gradual precipitation of SM-NZVI particles, this extension occurred intensively in the bottom of the zone, which also promoted the reduction of deep-seated NB. In addition, the upstream concentration was obviously higher than that of the downstream reactive area, indicating the dilution effect of inflow was less important as aforesaid, and the reduction of the zone with nanoiron was the principal cause of NB degradation.

The reactivity of nanoiron particles directly determines the effectiveness of the IRZ. It was found that the decrease in the NB concentration had slowed since the 40th day, and that the trailing concentration was steady at more than 100 mg/L. Considering the distribution of the IRZ, evidently the removal of nitrobenzene at the top, and end, of the box happened more slowly than in the bottom of the box. This disparity arose because the transport of NZVI particles has been proved to be quite limited, no greater than several metres, and accompanied by intense sedimentation that comes from aggregation and oxidation (Schrick *et al.* 2004).

Compared with the removal effect of NB in coarse sand, the results in fine sand were less efficient as shown in Figure 3. The reaction area was in the range of 15–60 cm on the 5th day, and the spreading rate of the zone was also relatively lower for the range of 20–80 cm by the 60th day. Many studies on NZVI transport in different media have demonstrated that the NZVI particles are adsorbed more strongly by media with a smaller size for a larger specific surface area, which naturally leads to their limited transport distances (Vasiliki &

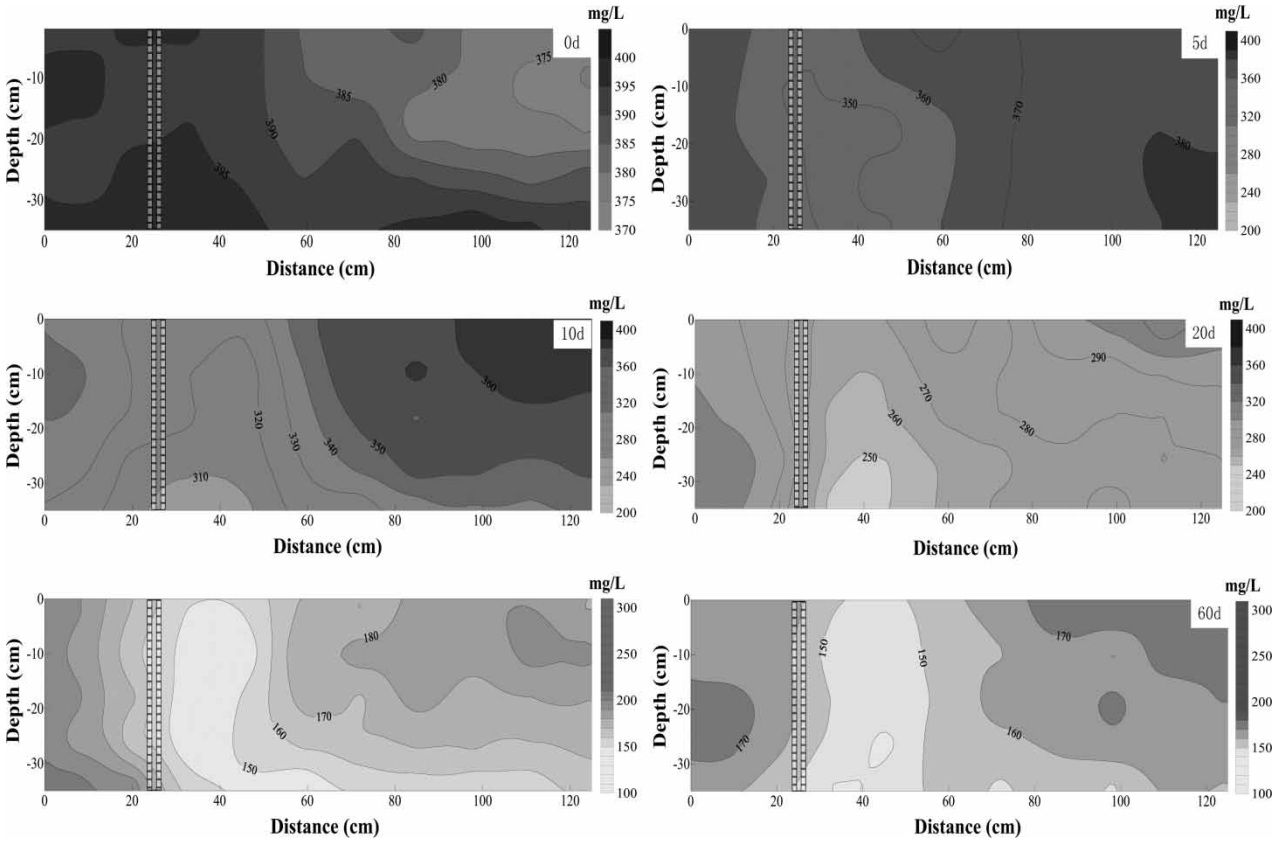

Figure 3 | Concentration change of nitrobenzene in fine sand.

Constantinos 2012). Therefore, the NB in the reactive zone with a higher NZVI concentration was degraded substantially, but the NB concentration for the distance range of 0–20 cm and 60–120 cm always stayed above 160 mg/L.

Given the above analyses and results, it may be concluded that the media size of the aquifer has an important influence on the remediation of NB in the IRZ with NZVI; or rather, NB is better removed in the media with larger size due to the wider range of the IRZ for relatively better transport of NZVI particles. On the other hand, the higher concentration of NZVI in a narrow area will lead to severe agglomeration of the nanoparticles, as well as the generation and attachment of oxidation products to the iron surface – both outcomes can further decrease the reactivity of NZVI particles.

Production effect of aniline in sand boxes

Prior studies have shown that nitrobenzene will be reduced to aniline, the end-product, by zero-valent iron (Huang *et al.* 2015). The spatio-temporal distributions of aniline in the aquifer boxes are shown in Figures 4 and 5. Clearly, after all the slurry was injected, less aniline was generated due to the limited transport of SM-NZVI in the first 5 days; hence, the reduced NB concentration away from the injection wells may be attributed to diluted slurry. As the reaction proceeded, the concentration of aniline in every area gradually increased until the reduction entered the trailing state. As seen in Figure 4, the average concentration of aniline in coarse sand was 24.74, 46.76, 84.89, and 97.02 mg/L on the 10th, 20th, 40th, and 60th day, which corresponded to a production rate – the ratio of an actual vs theoretical amount – of 46.3%, 38.2%, 59.8%, and 25.8%, respectively. Therefore, the area of the IRZ primarily expanded in the first 40 days, thus prolonging the contact time between NB and SM-NZVI, which promoted the transformation of NB into aniline.

The concentration changes of aniline in fine sand are shown in Figure 5. The average concentration of aniline

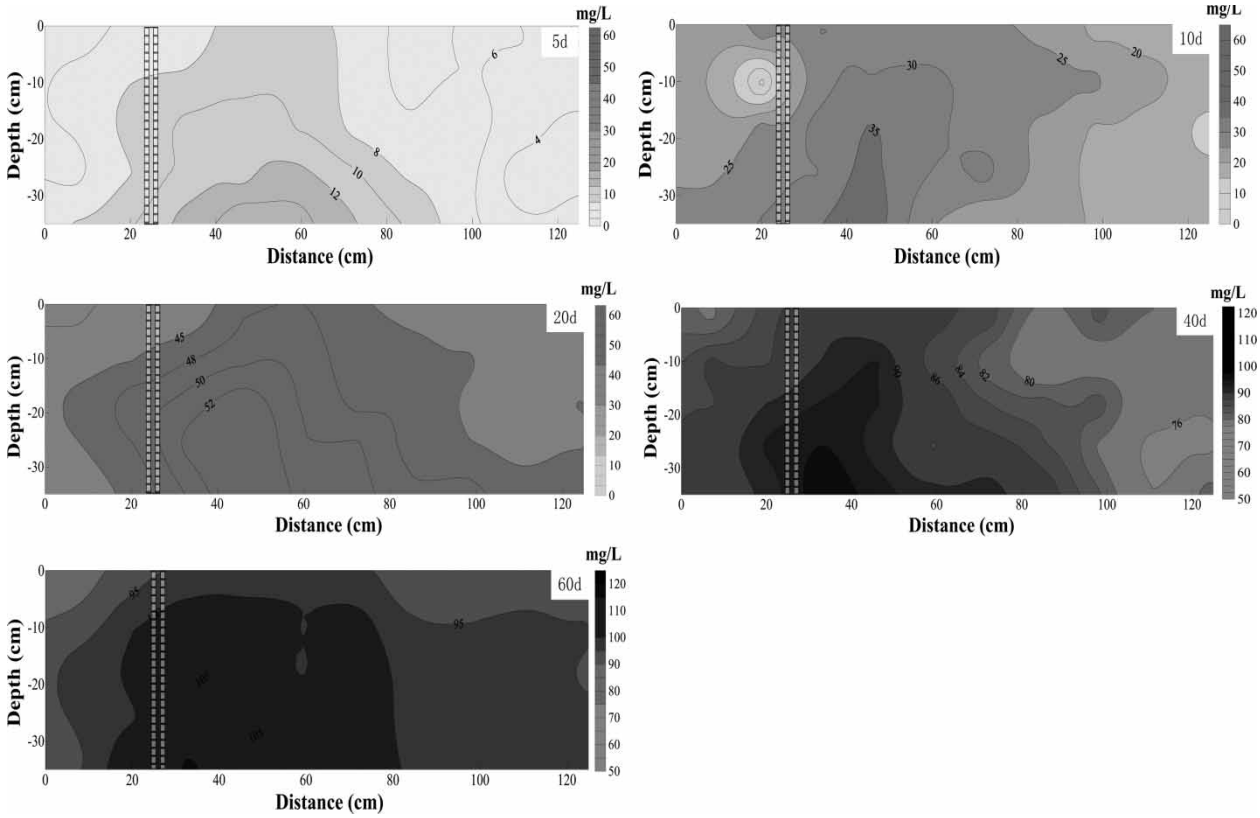

Figure 4 | Concentration change of aniline in coarse sand.

was 10.87, 24.67, 42.77, and 49.40 mg/L, with a corresponding production rate of 29.2%, 30.3%, 31.6%, and 18.4% on the 10th, 20th, 40th, and 60th day, respectively. Over the 2-month period, the average production rate was 1.93 times in coarse than that in fine sand (40.1% and 20.8%, respectively). Hence, for each time period considered, the production rate in fine sand was distinctly lower than that in coarse sand, a result explained by the more effective contact of nanoparticles and the pollutant in the aquifer containing media of a larger size. Some reports about NB degradation by zero-valent iron have drawn a similar conclusion: intermediate products, such as nitrosobenzene and hydroxylaniline, would be generated for inadequate contact, and these pollutants remain more toxic than aniline for the infeasibility of biodegradation. Therefore, not only NB reduction but also aniline production is related to the final remediation effect. How to improve the transport ability and sustainable reactivity of NZVI is the key to applications of IRZ technology.

The formation and development of the IRZ

Based on the above results and their analysis, the formation and development of the IRZ with NZVI may be summed up as the following process: a large area of IRZ in the flow direction is formed due to the transport of injected NZVI, and a small area of IRZ upriver with a lower concentration of NZVI is formed by head or mechanical pressure from the injection process. The IRZ is conspicuously heterogeneous, which is because the NZVI particles will continuously deposit on the surface of the aquifer media during the migration process, as well as settle deeply into the aquifer via gravity. Therefore, the removal efficiency of the target pollutant around the injection wells and deeper in the aquifer will likely exceed that elsewhere, and the efficiency will decrease with the distance from the wells.

Penetrability change of the IRZ

The water yield and level in the piezometer tubes were measured regularly, and the changing permeability

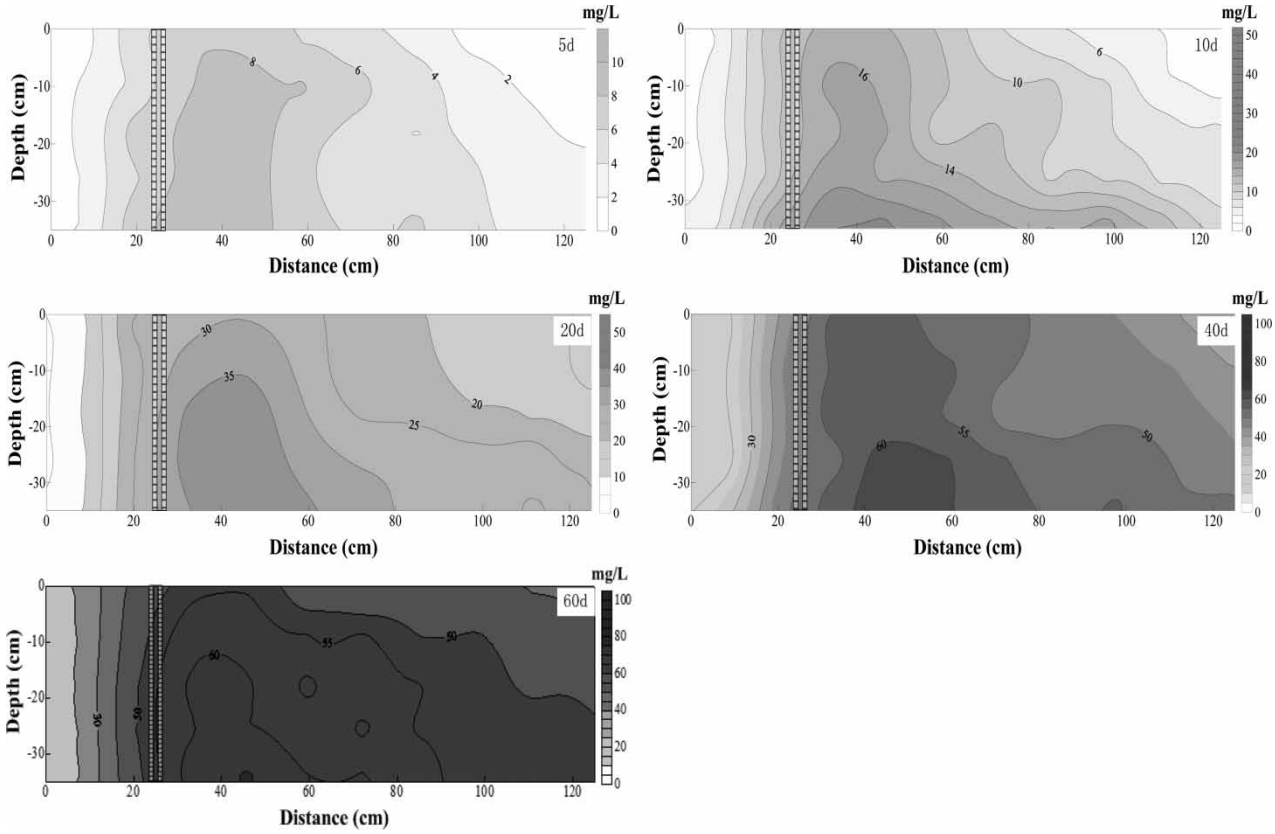

Figure 5 | Concentration change of aniline in fine sand.

coefficient was calculated according to the Darcy law. As shown by the curves in Figure 6, the initial water yield of the aquifer box was 18.8 and 11.7 mL/min for coarse and fine sand, respectively, but this quickly declined to 16.2 and 10.3 mL/min as the SM-NZVI slurry was injected. As the IRZ proceeded, the water yield tended to drop slowly, such that the final water yield stayed at c. 15and 9.2 mL/min, for coarse and fine sand respectively, representing a 20.2% and 12.0% decline when compared with the initial values. These results indicate that although the injection of NZVI slurry will reduce the water yield of the aquifer, there is little impact thereafter from the operation of the IRZ or the reduction reaction.

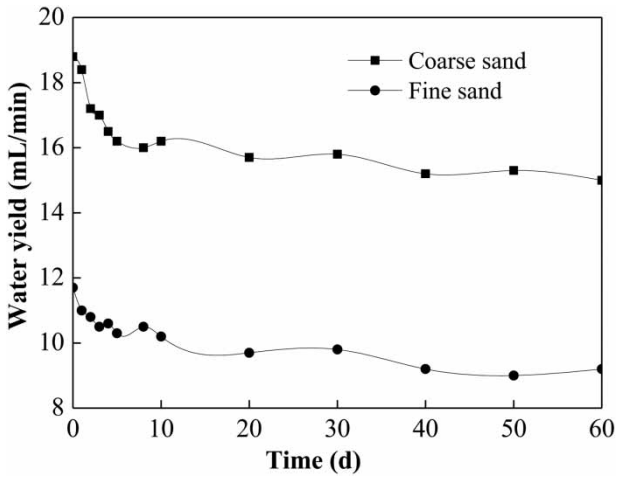

Figure 6 | Trends of water yield in coarse and fine sand.

The hydraulic gradient is one of the most important parameters when measuring the permeability change of an aquifer. It was calculated by recording the change of water level in piezometer tubes, named by their column number plus 'PT'. Take the results of NO.2, NO.4, and NO.8 PT, for example. As shown in Figure 7, the water level of NO.2 PT in both aquifers clearly increased during the first 10 days, indicating that the injection of the SM-NZVI slurry can significantly reduce the permeability of the

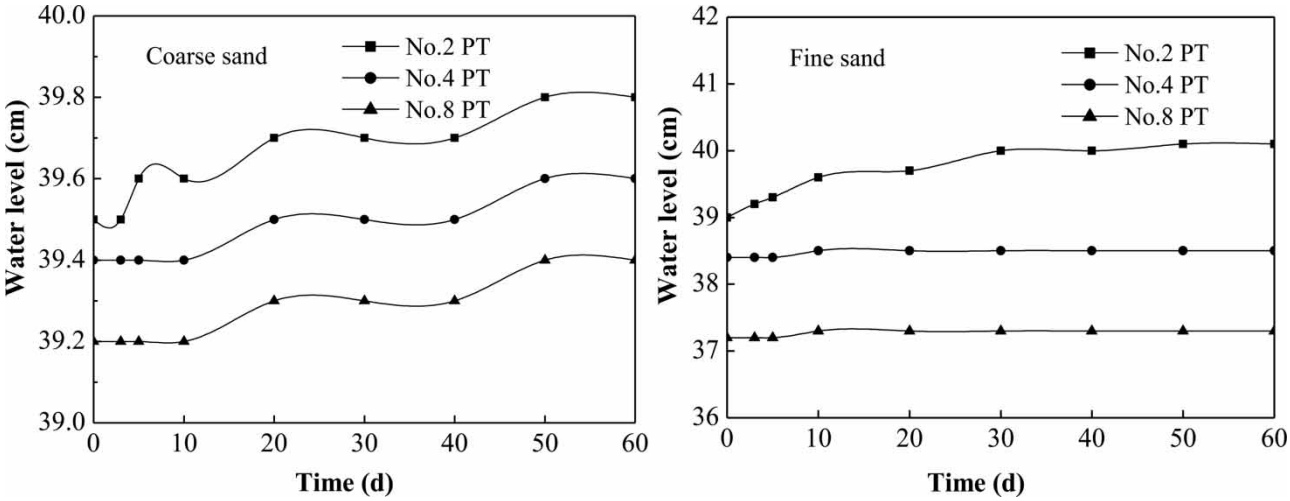

Figure 7 | Groundwater level variation of the piezometer tubes during the remediation process.

aquifer around the injection wells. After that, the water level in the coarse sand continued to increase though it remained stable in fine sand apart from NO.2 PT.

The increased water level was bound to change the hydraulic gradient in the aquifer. In the first 20 days, the hydraulic gradient between NO.2 and NO.4 PT gradually increased due to the slurry injection and the degradation of NB by nanoiron, and the corresponding permeability coefficient was reduced, respectively, from 56.12 to 22.94 m/d in coarse sand and from 5.79 to 4.96 m/d in fine sand (Figure 8). After 20 days, the permeability of this area in coarse sand seemed little changed, whereas it continuously decreased to 1.82 m/d in fine sand; this difference suggests that the reduction reaction had a smaller impact on the permeability with the increase of media size. Furthermore, it can be seen that the hydraulic gradient between NO.4 and NO.8 PT was nearly constant (Figure 7), likely because there were fewer NZVI particles transported to the area – which is farther from the injection wells – and so the decrease in permeability during the first 10 days was mainly caused by a change in water yield.

In summary, the injection of NZVI slurry reduced the permeability of the aquifer, though the permeability

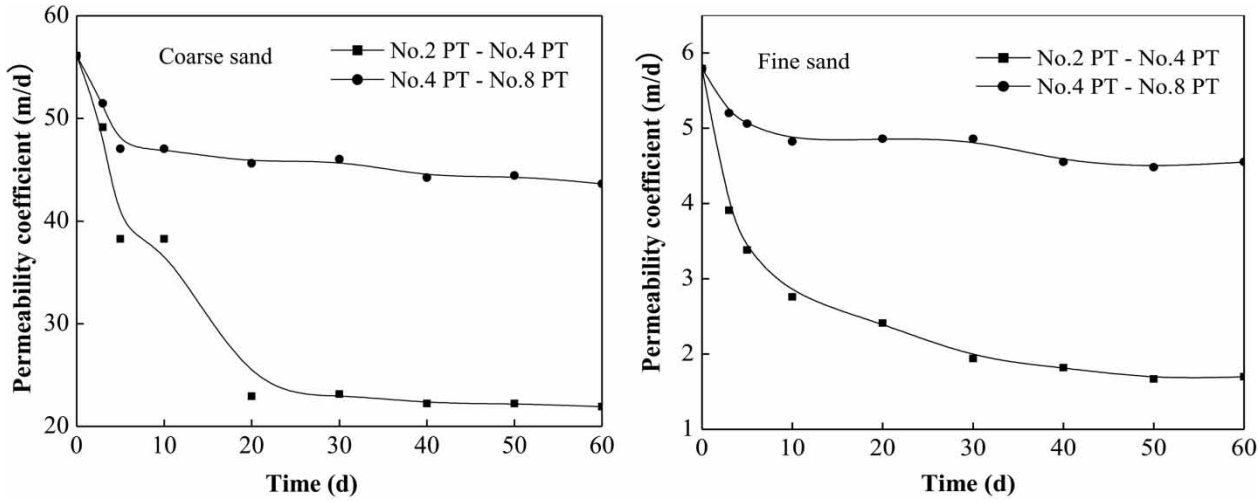

Figure 8 | Permeability variation of IRZ during the remediation process.

coefficient always kept in the same order of magnitude; that is, the slurry would not cause obvious changes to the groundwater flow field. As the IRZ or the reaction proceeded, both NB degradation and NZVI oxidation were also not likely to reduce the permeability of the aquifer significantly, let alone block the aquifer.

CONCLUSION

To investigate the remediation efficiency of an in-situ reactive zone with NZVI for nitrobenzene, a two-dimensional simulated experiment was undertaken in saturated porous media, and the removal efficiency of nitrobenzene and the production rate of aniline were described in detail, as was the permeability change of the aquifer. Based on the properties of NZVI particles and the data maps, the formation and development of an IRZ was easily discerned. The research findings are summarized as follows:

1. The media of the aquifer has an important effect on the formation of an IRZ. The area of the IRZ will increase with the media size of the aquifer, which enhances the remediation effect. In coarse and fine sand, the IRZ with SM-NZVI entered the trailing period on the 50th and 40th day, respectively, and the corresponding trailing concentration of NB was 87.24 and 170.24 mg/L. After 60 days, the average production rate of aniline had reached 40.1% and 20.8%.
2. The injection of SM-NZVI reduced the water yield by 13.8% and 11.9% in coarse and find sand, respectively. As the reaction progressed, the water yield basically remained stable, but the hydraulic gradient of the aquifer continued to increase, particularly in the reaction zone.
3. There was no sign of a blockage in the aquifer, although the permeability declined, by 60.9% and 70.6%, with the injection of NZVI slurry (to 22.94 and 1.82 m/d, respectively).
4. The formation and remediation ability of the IRZ with NZVI is heterogeneous: the concentration and degradation ability of the IRZ will decrease with distance from the injection wells, and a better removal efficiency for pollutants at the bottom of the zone is predicted because of the precipitation there of the NZVI particles.

ACKNOWLEDGEMENTS

This study was funded by the Natural Science Foundation of China (No. 41602269), the Basal Research Fund of the Chinese Academy of Geological Sciences (No. YYWF201629), and the Natural Science Foundation of Hebei Province (No. D2017504004).

REFERENCES

Adeleye, A. S., Keller, A. A., Miller, R. J. & Lenihan, H. S. 2013 Persistence of commercial nanoscaled zero-valent iron (nZVI) and by-products. *Journal of Nanoparticle Research* **15**, 1418.

Dong, T. T., Luo, H. J. & Wu, J. H. 2010 Preparation of nanoscale zero-valent iron particles and its application in *p*-nitrochlorobenzene degradation in wastewater. *Chinese Journal of Environmental Engineering* **4** (6), 1257–1261.

Dong, J., Wen, C. Y., Liu, D., Zhang, W., Li, J., Jiang, H., Qin, C. & Hong, M. 2015 Study on degradation of nitrobenzene in groundwater using emulsified nano-zero-valent iron. *Journal of Nanoparticle Research* **17**, 31.

Dubey, A., Mishra, A., Min, J. W., Lee, M. H., Kim, H., Stang, P. J. & Chi, K. 2014 Self-assembly of new arene-ruthenium rectangles containing triptycene building block and their application in fluorescent detection of nitro aromatics. *Inorganica Chimica Acta* **423**, 326–331.

Elliott, D. W. & Zhang, W. X. 2001 Field assessment of nanoscale bimetallic particles for groundwater treatment. *Environmental Science and Technology* **35**, 4922–4926.

Grube, M., Muter, O., Strikauska, S., Gavare, M. & Limane, B. 2008 Application of FT-IR spectroscopy for control of the medium composition during the biodegradation of nitro aromatic compounds. *Journal of Industrial Microbiology & Biotechnology* **35**, 1545–1549.

Guria, M. K., Majumdar, M. & Bhattacharyya, M. 2016 Green synthesis of protein capped nano-gold particle: an excellent recyclable nano-catalyst for the reduction of nitro-aromatic pollutants at higher concentration. *Journal of Molecular Liquids* **222**, 549–557.

Han, Y., Shi, N., Wang, H., Pan, X., Fang, H. & Yu, Y. 2016 Nanoscale zerovalent iron-mediated degradation of DDT in soil. *Environmental Science and Pollution Research* **223**, 6253–6263.

He, F. & Zhao, D. 2005 Preparation and characterization of a new class of starch-stabilized bimetallic nanoparticles for degradation of chlorinated hydrocarbons in water. *Environmental Science and Technology* **39**, 3314–3320.

Higgins, M. R. & Olson, T. M. 2009 Life-cycle case study comparison of permeable reactive barrier versus pump-and-treat remediation. *Environmental Science and Technology* **43**, 9432–9438.

Huang, D., Chen, G., Zeng, G., Xu, P., Yan, M., Lai, C., Zhang, C., Li, N., Cheng, M., He, X. & He, Y. 2015 Synthesis and application of modified zero-valent iron nanoparticles for removal of hexavalent chromium from wastewater. *Water, Air, and Soil Pollution* **226**, 375.

Kulkarni, M. & Chaudhari, A. 2007 Microbial remediation of nitro-aromatic compounds: an overview. *Journal of Environmental Management* **85**, 496–512.

Li, H., Zhao, Y. S., Zhao, R., Ma, B., Chen, Z., Su, Y. & Zhou, R. 2013 Characteristics and kinetics of nitrobenzene reduction by sucrose-modified nanoiron. *Chemical Research in Chinese Universities* **29**, 765–770.

Lin, L., Xu, B., Lin, Y. L., Yan, L., Shen, K. Y., Xia, S. J., Hu, C. Y. & Rong, R. 2013 Reduction of *n*-nitrosodimethylamine (NDMA) in aqueous solution by nanoscale $Fe/Al_2(SO_4)_3$. *Water, Air, and Soil Pollution* **224**, 1632.

Liu, D., Thomson, K. & Strachan, W. M. J. 1981 Biodegradation of carbaryl in simulated aquatic environment. *Bulletin of Environmental Contamination and Toxicology* **27**, 412–417.

Ponder, S. M., Darab, J. G. & Mallouk, T. E. 2000 Remediation of Cr(VI) and Pb(II) aqueous solutions using supported, nanoscale zero-valent iron. *Environmental Science and Technology* **34**, 2564–2569.

Rezaei-Vahidian, H., Zarei, A. R. & Soleymani, A. R. 2017 Degradation of nitro-aromatic explosives using recyclable magnetic photocatalyst: catalyst synthesis and process optimization. *Journal of Hazardous Materials* **325**, 310–318.

Schlicker, O., Ebert, M., Fruth, M., Weidner, M., Wüst, W. & Dahmke, A. 2000 Degradation of TCE with iron: the role of competing chromate and nitrate reduction. *Groundwater* **38**, 403–409.

Schrick, B., Hydutsky, B. W., Blough, J. L. & Mallouk, T. E. 2004 Delivery vehicles for zerovalent metal nanoparticles in soil and groundwater. *Chemistry of Materials* **16**, 2187–2193.

Suthersan, S. S. 2002 *Natural and Enhanced Remediation Systems*. Lewis Publishers, Boca Raton, FL, USA.

Tiraferri, A. & Sethi, R. 2009 Enhanced transport of zerovalent iron nanoparticles in saturated porous media by guar gum. *Journal of Nanoparticle Research* **11**, 635–645.

Vasiliki, I. S. & Constantinos, V. C. 2012 Transport of biocolloids in water saturated columns packed with sand: effect of grain size and pore water velocity. *Journal of Contaminant Hydrology* **126**, 301–314.

Yan, J., Ni, J., Zhao, J., Sun, L., Bai, F., Shi, Z. & Xing, Y. 2017 The nitro aromatic compounds detection by triazole carboxylic acid and its complex with the fluorescent property. *Tetrahedron* **73**, 2682–2689.

Yin, W. Z., Wu, J. H., Huang, W. L. & Wei, C. H. 2015 Enhanced nitrobenzene removal and column longevity by coupled abiotic and biotic processes in zero-valent iron column. *Chemical Engineering Journal* **259**, 417–423.

Yuan, B. L., Chen, Y. M. & Fu, M. L. 2012 Degradation efficiencies and mechanisms of trichloroethylene (TCE) by controlled-released permanganate (CRP) oxidation. *Chemical Engineering Journal* **192**, 276–283.

Yuan, B. L., Li, F., Chen, Y. M. & Fu, M. L. 2013 Laboratory-scale column study for remediation of TCE-contaminated aquifer using three-section controlled-release potassium permanganate (CRP) barriers. *Journal of Environmental Sciences* **25** (5), 971–977.

Zhou, Z. M., Ruan, W. J., Huang, H. S., Shen, C. H., Yuan, B. L. & Huang, C. H. 2015 Fabrication and characterization of Fe/Ni nanoparticles supported by polystyrene resin for trichloroethylene degradation. *Chemical Engineering Journal* **283**, 730–739.

First received 10 August 2017; accepted in revised form 26 January 2018. Available online 13 February 2018